Available online at www.sciencedirect.com

SCIENCE DIRECT®

Developmental Biology 272 (2004) 339–350

DEVELOPMENTAL BIOLOGY

www.elsevier.com/locate/ydbio

The role of mechanical forces in dextral rotation during cardiac looping in the chick embryo

Dmitry A. Voronov,[a,b] Patrick W. Alford,[a] Gang Xu,[a] and Larry A. Taber[a,*]

[a] *Department of Biomedical Engineering, Washington University, St Louis, MO 63130, USA*
[b] *Institute for Information Transmission Problems, Russian Academy of Sciences, Moscow, Russia*

Received for publication 1 December 2003, revised 4 March 2004, accepted 7 April 2004
Available online 24 June 2004

Abstract

Cardiac looping is a vital morphogenetic process that transforms the initially straight heart tube into a curved tube normally directed toward the right side of the embryo. While recent work has brought major advances in our understanding of the genetic and molecular pathways involved in looping, the biophysical mechanisms that drive this process have remained poorly understood. This paper examines the role of biomechanical forces in cardiac rotation during the initial stages of looping, when the heart bends and rotates into a c-shaped tube (c-looping). Embryonic chick hearts were subjected to mechanical and chemical perturbations, and tissue stress and strain were studied using dissection and fluorescent labeling, respectively. The results suggest that (1) the heart contains little or no intrinsic ability to rotate, as external forces exerted by the splanchnopleure (SPL) and the omphalomesenteric veins (OVs) drive rotation; (2) unbalanced forces in the omphalomesenteric veins play a role in left–right looping directionality; and (3) in addition to ventral bending and rightward rotation, the heart tube also bends slightly toward the right. The results of this study may help investigators searching for the link between gene expression and the mechanical processes that drive looping.

Keywords: Avian embryo; Cardiac morphogenesis; Heart development; Left–right asymmetry; Biomechanics

Introduction

Cardiac looping is the first visible morphologic indication of left–right asymmetry in vertebrate embryos. Because abnormal looping can lead to congenital heart defects, this process has received considerable attention for many years. It is now known that looping directionality correlates with asymmetric expression of several genetic and molecular markers (Brand, 2003; Harvey, 1998; Mercola and Levin, 2001; Srivastava and Olson, 1997), but the biophysical mechanisms that drive looping remain poorly understood (Manner, 2000; Taber et al., 1995). This paper examines the role of biomechanical forces in rightward (dextral) rotation of the primitive heart tube.

As looping direction is apparently determined relatively early in development, most studies have focused on the initial phase of looping, called c-looping, when the initially straight heart tube deforms into a c-shaped tube that is normally curved toward the right side of the embryo. Labeling experiments have shown that normal c-looping consists of two main deformation components: ventral bending and rightward rotation (Fig. 1) (Manner, 2000).[1] Several studies have suggested that the bending component is regulated by forces intrinsic to the heart tube (Butler, 1952; Manning and McLachlan, 1990), and some investigators have speculated that rotation is also caused by internal forces (Itasaki et al., 1991; Manasek et al., 1984). Recently, however, we have found that the splanchnopleure (SPL), a membrane that pushes against the heart tube, causes considerable heart rotation in the chick embryo (Voronov and Taber, 2002).

* Corresponding author. Department of Biomedical Engineering, Washington University, Campus Box 1097, St. Louis, MO 63130. Fax: +1-314-935-7448.
E-mail address: lat@wustl.edu (L.A. Taber).

[1] Because the ends of the cardiac tube are relatively fixed, rotation involves twisting deformation near the ends of the ventricle. Rotation is the term used most often to describe this phenomenon, but twist describes the deformation more precisely in mechanical terms. Hence, "rotation" and "twist" are used interchangeably in this paper.

0012-1606/$ - see front matter © 2004 Elsevier Inc. All rights reserved.
doi:10.1016/j.ydbio.2004.04.033

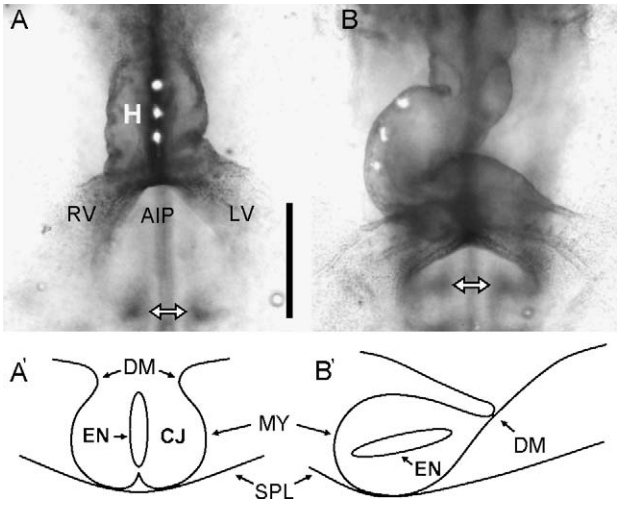

Fig. 1. C-looping in normal chick embryo, ventral view. (A) Straight heart tube at stage 10 (9 somites) with fluorescent labels along ventral midline. (B) Same embryo 6 h later with labels on the outer curvature indicating heart rotation toward the right. (A′ and B′) Schematic transverse sections of above hearts near midventricle. AIP, anterior intestinal portal; CJ, cardiac jelly; DM, dorsal mesocardium; EN, endocardium; H, heart tube; LV, RV, left, right omphalomesenteric vein; MY, myocardium; SPL, splanchnopleure. Double-headed arrows in A and B indicate the first pair of somites. Note movement of AIP in the caudal direction. Scale bar: 400 μm.

Using both experimental and computational models, we herein examine further the mechanical forces involved in the rotational component of c-looping. The results suggest that (1) the heart contains little or no intrinsic ability to rotate, as external forces due primarily to the splanchnopleure (SPL) and secondarily to the omphalomesenteric veins (OVs) drive rotation; (2) unbalanced forces in the OVs play a role in left–right looping directionality; and (3) in addition to ventral bending and rightward rotation, the heart tube also bends slightly toward the right. We feel that these results provide a better understanding of the biophysical mechanisms that regulate cardiac c-looping.

Materials and methods

Fertilized White Leghorn chicken eggs were incubated for approximately 30–35 h in a humidified atmosphere at 38°C to yield embryos at stages 9–10 of Hamburger and Hamilton (1951). Embryos were extracted from the eggs using Whatman #2 filter paper rings (Chapman et al., 2001; Flynn et al., 1991; Voronov and Taber, 2002) and washed in chick Ringer's solution (0.7% NaCl, 0.037% KCl, 0.018% $CaCl_2$ in distilled water). All dissections were performed using fine glass needles made from pulled micropipettes.

Embryo culture

Two techniques of embryo culture were used. One was a variation of the method of New (1955), with the embryo placed on the surface of semisolid medium. In the other method, the embryo was placed under a thin layer of liquid medium. Unless stated otherwise, all results presented in this paper are based on the second method, which eliminates potential artifact due to surface tension (Voronov and Taber, 2002).

For the first culture method, semisolid medium was prepared by mixing equal volumes of warm egg albumen and 0.3% agar in chick Ringer's solution with 1% antibiotics (penicillin–streptomycin–neomycin, Gibco BRL #15640) added (Chapman et al., 2001; Flynn et al., 1991; Voronov and Taber, 2002). An approximately 2 mm layer of medium was added to 35 or 60 mm Petri dishes, and an embryo on a paper ring was placed ventral side up on the agar. The embryos were developed in an incubator (Queue Systems, Inc, Model QMI300SABA) with a 5% CO_2 atmosphere at 38°C.

For the second culture method, liquid medium was prepared by mixing 89% Dulbecco's modified Eagle's medium (DMEM) (Sigma, D1152), 10% chick serum (Sigma, C5405), and 1% antibiotics (Voronov and Taber, 2002). An embryo fixed between two filter paper rings was placed ventral side up in a Petri dish and then covered by the liquid medium to a depth of approximately 0.5 mm above the heart. To avoid floating of the embryo and to hold it between the paper rings, a stainless steel ring (diameter 20–22 mm, wire cross-section 1 mm) was placed on the upper paper ring before the medium was added. Petri dishes containing embryos were then placed in 12 × 20 cm plastic bags ("Ziploc") filled with a mixture of 95% O_2 and 5% CO_2, and then the sealed bags were put into an incubator. Several drops of water were added to the bags to increase humidity.

Tissue labeling and imaging

Cells or small groups of cells in the myocardium were labeled with the fluorescent dye DiI (Molecular Probes, D-282) or DiO (Molecular Probes, D-275) mixed in sucrose solution (Bronner-Fraser, 1996). Dye was injected through glass micropipettes via a pneumatic pump (PicoPump PV830, World Precision Instruments). The heart was labeled by piercing the SPL, leaving this membrane otherwise intact.

In one set of experiments, fluorescent staining of the actin cytoskeleton was used to help visualize the edges of myocardial cuts. Embryos were fixed overnight with 4% formaldehyde in PBS (pH 7.2). Then, the embryos were washed for 1 h in PBS with 10% bovine albumin (Sigma, A8327) and 0.1% Triton X-100 (Sigma), and the actin was stained 1 h with 0.3 M rhodamine-labeled phalloidin (Molecular Probes, R-415).

Fluorescent and bright-field illuminated pictures were taken with a video camera (Retiga 1300) installed on a fluorescent microscope (Leica DMLB) or with a CCD camera (COHU, Model 4915) mounted on dissecting microscope (Leica MZ8). Images were processed using Adobe Photoshop and ImageJ programs.

Chemical perturbations

For global actin perturbation, 2 μM cytochalasin B (Sigma) was dissolved in DMSO and added to the culture media. For local perturbation, a crystal of cytochalasin B was placed next to the heart through a small hole cut in the SPL.

Statistics

Statistical analysis was performed using SigmaStat software (SPSS, Chicago, IL).

Computational model

A model for the stage 10 heart was created using the commercial finite element code ABAQUS (v. 6.3, Abaqus, Inc.). As a first approximation, the ventricle is modeled as a straight tube consisting of a thin layer of myocardium surrounding a relatively thick layer of cardiac jelly (see Fig. 9A). The lower end of the ventricle is fixed to the OVs, which are represented by curved tubes with cross sections similar to that of the ventricle. Consistent with the morphology (Fig. 1A), the left vein has a larger diameter than the right vein. The dorsal side of the ventricle is attached to myocardial extensions representing the dorsal mesocardium, which is fixed along its dorsal side. The far ends of the OVs are also fixed.

For modeling morphogenesis, growth and contractile stresses were included in ABAQUS through the user-supplied subroutine UMAT, which can be used to prescribe custom nonlinear material properties. Here, we provide a brief overview of the method, which is based on our general theory for the biomechanics of development (Taber, 2001).

Extending the growth theory of Rodriguez et al. (1994), we model growth and contraction by changing the zero-stress configuration for each material element. Relative to the current zero-stress configuration, each element grows and contracts (activates) according to deformation gradient tensors $\boldsymbol{F}_g$ and $\boldsymbol{F}$, respectively, and then stresses induce the additional elastic deformation $\boldsymbol{F}$. Hence, the total deformation is described by $\boldsymbol{F} = \boldsymbol{F}_e\boldsymbol{F}_a\boldsymbol{F}_g$, where $\boldsymbol{F}_g = \boldsymbol{I}$ for no net growth and $\boldsymbol{F}_a = \boldsymbol{I}$ for passive tissue. ($\boldsymbol{I}$ is the identity tensor.) In material constitutive relations, stress depends only on the local elastic deformation $\boldsymbol{F}_e$.

To a first approximation, we assume that myocardium and cardiac jelly are isotropic, incompressible, pseudoelastic materials characterized by the strain-energy density function $W = C(I_1 - 3)$, where I_1 is the first invariant of the elastic strain tensor $\boldsymbol{E}_e = (\boldsymbol{F}_e^T\ \boldsymbol{F}_e - \boldsymbol{I})/2$, and C is a material constant. From the measurements of Zamir et al. (2003), we take $C = 30$ Pa for myocardium and precardiac cells in the OVs, and $C = 3$ Pa for cardiac jelly.

In this model, the tensors $\boldsymbol{F}_g$ and $\boldsymbol{F}_a$ are specified functions of time. Let the unit vectors $\boldsymbol{e}_1$, $\boldsymbol{e}_2$, and $\boldsymbol{e}_3$ be

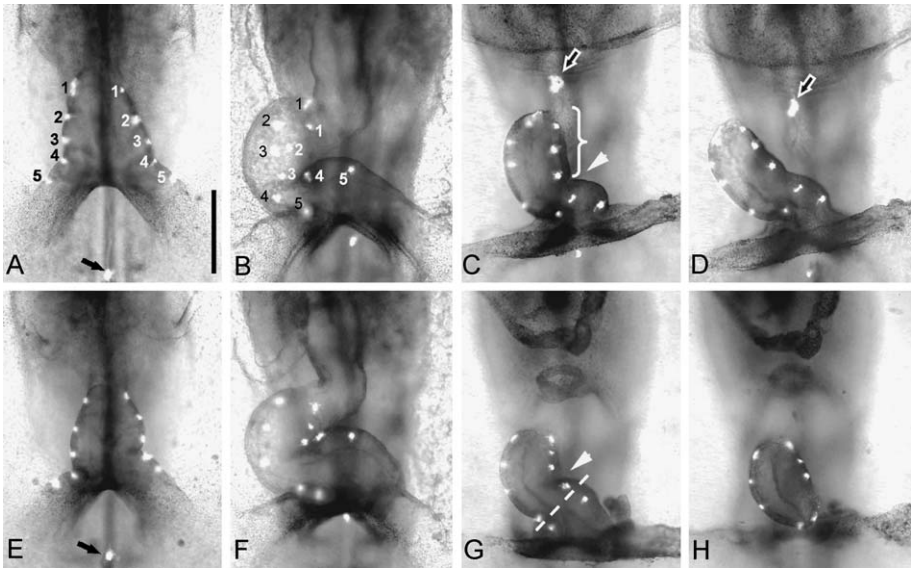

Fig. 2. Effect of external forces on c-looping for two embryos (A–D and E–H). (A and E) Intact stage 10 hearts with labels along the left and right sides of ventricle and between the first pair of somites (arrow). (B and F) Same hearts at stage 11 after 6 h of cultivation; as the heart rotates rightward, labels move toward dorsal and ventral sides. Note that the labels on the dorsal side (black numbers) are seen through the transparent heart tube and, therefore, are surrounded by a halo of dispersed light. (C and G) Same hearts 30 min after removal of splanchnopleure; most rotation disappears as heart untwists, but heart remains bent toward the right. (D) Heart in C after transverse cutting of conotruncus and longitudinal cutting of dorsal mesocardium (bracket = length of cut). (H) Heart in G after removal of caudal end of heart and omphalomesenteric veins (below dashed line). After 30 min of culture, the label positions in D and H indicate that the remainder of the rotation is lost, and the heart unbends but remains slightly bent toward the right. In addition, the interventicular groove (C and G arrowheads) smoothes out as the heart unbends (D and H). (Black and white arrows in C and D indicate label on conotruncus above the cut.) Scale bar: 400 μm.

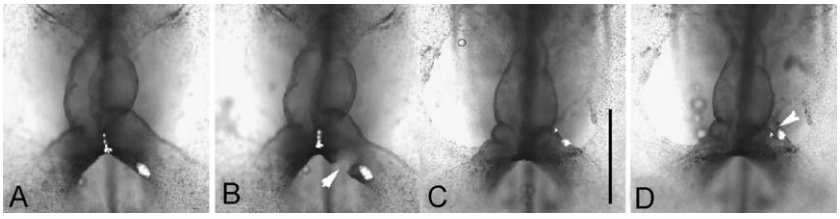

Fig. 3. Stresses in embryonic heart. (A and C) Stage 10 embryos with labels on left omphalomesenteric vein. (B and D) Same hearts immediately after small cuts are made between each pair of labels. Labels on caudal side move apart and wound opens (arrowhead in B), indicating local tension. Labels on cranial side move slightly closer (arrowhead in D), indicating local compression. Scale bar: 400 μm.

directed along the local longitudinal, circumferential, and radial directions, respectively, in the heart tube or OVs. For a first approximation, we take $\boldsymbol{F}_g = \lambda_{g1}\boldsymbol{e}_1\boldsymbol{e}_1 + \lambda_{g2}\boldsymbol{e}_2\boldsymbol{e}_2 + \lambda_{g3}\boldsymbol{e}_3\boldsymbol{e}_3$ and $\boldsymbol{F}_a = \lambda_{a1}\boldsymbol{e}_1\boldsymbol{e}_1 + \lambda_{a2}\boldsymbol{e}_2\boldsymbol{e}_2 + \lambda_{a3}\boldsymbol{e}_3\boldsymbol{e}_3$, where the λs are stretch ratios (Taber, 2001; Taber and Perucchio, 2000). Morphogenetic mechanisms are simulated as follows:

- Actin polymerization in heart tube: as described later, λ_{g1} or λ_{g2} increases from 1 to 1.3 along the principal actin fiber directions with no change in material properties.
- Cytoskeletal contraction in OVs: during activation, λ_{a1} decreases linearly in time from 0.85 (initial contraction at stage 10) to 0.7 after 18 h, with C increasing to $30/\lambda_{a1}$ Pa. For constant cell volume ($\lambda_{a1}\ \lambda_{a2}\ \lambda_{a3} = 1$), we take $\lambda_{a2} = (\lambda_{a1})^{-1}$ and $\lambda_{a3} = 1$.
- Precardiac cell migration in OVs: influx of cells into the OVs is modeled by growth ($\lambda_{g1} > 1$) in the local longitudinal vein direction with no change in material properties.

Regional distributions of $\boldsymbol{F}_g$ and $\boldsymbol{F}_a$ are specified in the model according to experimental observations (see Results).

During each iteration in ABAQUS, all components of $\boldsymbol{F}$ at the beginning and end of the time increment are passed into UMAT for computing components of the stress and elasticity matrices, which are then passed back into the main program for equilibrium analysis. To include contraction and growth, we calculate $\boldsymbol{F}_e = \boldsymbol{F}\,\boldsymbol{F}_g^{-1}\,\boldsymbol{F}_a^{-1}$, which is used to compute the stress components.

Results

Effects of removing splanchnopleure and omphalomesenteric veins

The effects of removing external constraints from the looping heart are illustrated in Fig. 2. Fluorescent labels were injected along the left and right sides of the hearts of 23 stage 10 embryos (Figs. 2A and E), and the embryos, with intact SPL, were returned to the incubator. After 6 h in culture, the heart had looped into the form of a stage 11 heart, sending the labels from the original left and right sides to the ventral and dorsal surfaces of the heart tube, respectively (Figs. 2B and F). At this time, the SPL was removed. After an additional 30 min of culture, the heart tube untwisted, as indicated by movement of the labels back toward the left and right edges of the heart in the ventral view (Figs. 2C and G). With most of the rotation now gone, a rightward bending of the heart could be clearly seen (relative to the heart). Finally, either the conotruncus and dorsal mesocardium were cut ($n = 10$) to free the cranial end of the heart (Fig. 2D), or the OVs were cut ($n = 12$) to free the caudal end (Fig. 2H). In both cases, the remainder of the rotation was lost within 30 min, and the rightward bending of the heart tube decreased.

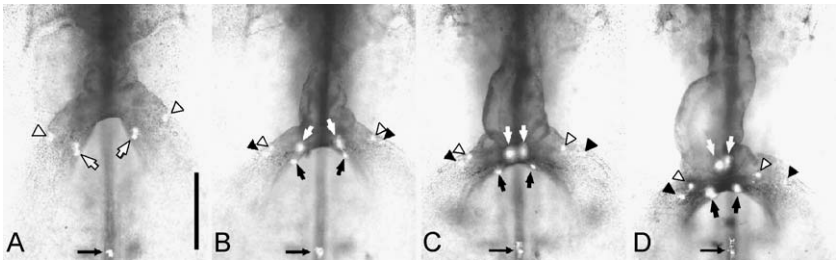

Fig. 4. Tissue migration in embryonic heart. (A) Stage 10 heart with labels in cranial (arrowheads) and caudal (arrows) regions of omphalomesenteric veins; both the endodermal and mesodermal layers are stained at each location. The first pair of somites is also labeled (thin black arrow). Label movements are shown after 2 (B), 4 (C), and 6 (D) h of cultivation. Black arrows and arrowheads indicate labels in the endoderm; white ones indicate labels in the underlying mesoderm. Both the endoderm and mesoderm move toward the midline, but the mesoderm migrates faster, splitting the labels. Due to fusion of the veins along the midline, the anterior intestinal portal moves caudally, but the caudal mesodermal labels (white arrows) remain approximately the same distance from the somites. Scale bar: 400 μm.

However, in addition to the bending toward its ventral side (as seen Figs. 2B and F), the heart remained bent slightly toward its right side (Figs. 2D and H).

Mechanical stresses in omphalomesenteric veins

The stresses in the SPL were explored in an earlier report (Voronov and Taber, 2002). Although the OVs cause much less rotation than the SPL (Fig. 2), we will show later that their contribution may be no less important. Hence, we examined the nature of the stresses in these veins.

Longitudinal stresses in the OVs were determined qualitatively using tissue dissection (Beloussov, 1998; Beloussov et al., 1975). Pairs of fluorescent labels were placed in the cranial and caudal regions of the OVs of stage 10 embryos, and small cuts were made between each pair of labels through small holes in the SPL. Immediately after cutting, the labels on the caudal sides moved apart, indicating longitudinal tension (Figs. 3A and B). The tension was large enough to cause considerable separation of the edges of the cut. In contrast, the labels on the cranial sides moved slightly closer together, indicating longitudinal compression in this region (Figs. 3C and D). Another indication of the compression in the veins, as well as in the heart tube, are wrinkles that are often seen in the stage 10 heart (e.g., see Figs. 1A, 4A, B, and 6A).

In all embryos ($n > 50$), the results consistently showed that the cranial and caudal regions of both OVs are in states of longitudinal compression and tension, respectively. It is possible, however, that the mesodermal and endodermal layers contribute differently to these apparent stresses. This issue warrants future study.

Tissue displacements in omphalomesenteric veins

Stresses in the OVs can be generated by several mechanisms, including cell migration and cytoskeletal contraction. It is known that precardiac mesoderm migrates as an epithelial sheet toward the caudal end of the heart tube during looping (de la Cruz, 1998), and contraction is a prominent feature of epithelial morphogenesis (Ettensohn, 1985; Schock and Perrimon, 2002; Wessells et al., 1971). To gain insight into which mechanisms contribute to OV stresses, we studied regional tissue displacements via labeling.

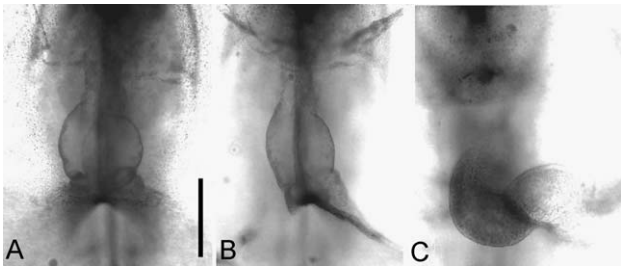

Fig. 5. Effects of removing right omphalomesenteric vein. (A) Intact stage 10 heart. (B) Same heart immediately after removing splanchnopleure and right vein; caudal end of ventricle displaces slightly toward the left. (C) After 18 h in culture (approximately stage 12), caudal end of heart tube is displaced toward the right. Scale bar: 400 μm.

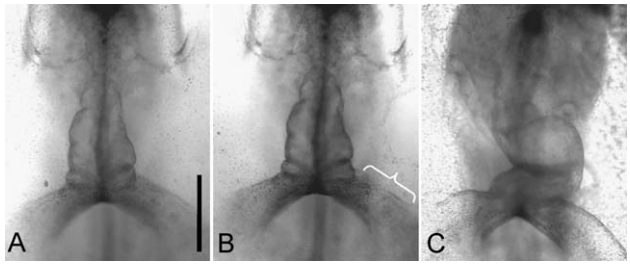

Fig. 6. Effect on looping of reducing force exerted by left omphalomesenteric vein. (A) Intact stage 10^{+} heart. (B) Same heart with part of the left vein removed by dissection (bracket), leaving the splanchnopleure intact. (C) Same heart 6 h later; left looping is observed. Scale bar: 400 μm.

Fluorescent labels were injected ventrally on the cranial and caudal sides of both OVs of 14 stage 10 embryos (Fig. 4A), staining both the endodermal and mesodermal layers of the veins at each point. (Relative to the ventral side of the embryo, the mesoderm lies below the endoderm.) Shortly after injection, each label splits, with the portion of the label in the mesoderm moving toward the heart tube, leaving its corresponding endoderm label behind (Figs. 4B–D). This behavior is consistent with the hypothesis that precardiac mesoderm migrates into the heart using the endoderm as a substrate (Linask and Lash, 1986, 1988a). All labels on the caudal side of the OVs moved faster than those on the cranial side. In fact, labels on the caudal side of the OV mesoderm moved all the way to the dorsal midline of the heart tube, in the region where the OVs merge to form the primitive atrium (Figs. 4C and D, white arrows).

It is important to note that the distance between mesoderm labels in the caudal regions of the OVs and a "fixed" label between the first pair of somites decreased only slightly (Figs. 4A–D). This observation supports the concept that the OVs progressively merge in a cranial to caudal direction during looping (de la Cruz and Sanchez-Gomez, 1998; Markwald et al., 1998). In other words, the apparent movement of these labels cranially into the heart tube is an illusion, as fusion of the OVs adds segments to the tube below the labels.

Global exposure to 2 μM cytochalasin B altered these displacements dramatically ($n = 31$). In fact, within 30 min, labels placed on the caudal side of the OVs moved considerably away from the heart, rather than toward it (results not shown, but see Figs. 7E and H for a similar response). Because cytochalasin B at this concentration inhibits actin polymerization and disrupts the actin cytoskeleton (Cooper, 1987; Wakatsuki et al., 2001), global exposure should inhibit both contraction and polymerization-driven cell migration. Loss of migration may decrease the compression on the cranial sides of the OVs,

but the increased distance between the labels suggests relaxation of longitudinal contractile stress on the caudal side.

Relative forces in omphalomesenteric veins

The stresses in the OVs exert net forces on the caudal end of the heart tube. Rightward displacement and rotation of the heart could be caused by the left vein pushing or the right vein pulling the heart. To determine whether the veins push or pull, we removed the SPL and dissected the right OV from two stage 10 embryos (Fig. 5). Immediately after the vein was removed, the left OV pulled the caudal end of the heart tube slightly leftward (Fig. 5B). After 18 h in culture, however, the left vein had pushed the heart considerably toward the right (Fig. 5C). Removing the left OV resulted in a similar, but oppositely directed response ($n = 2$, results not shown). These results indicate that net tensions in both OVs, possibly due to cytoskeletal contraction, initially pull on the heart. Later, however, both OVs push against the heart tube, possibly due to cell migration. The relative motions of the heart and OVs during normal looping (Fig. 1) suggest that the left vein pushes with greater force.

In another set of experiments, we investigated the effects of altering the balance of forces in the OVs. To reduce the force in the left OV of stage 10 embryos, we inserted a glass needle through a small hole in the SPL and carefully dissected out a segment of the vein (Figs. 6A and B). After 6 h in culture, 27% (6/22) of the treated hearts had looped to the left (Fig. 6C). Compared to control hearts, in which right

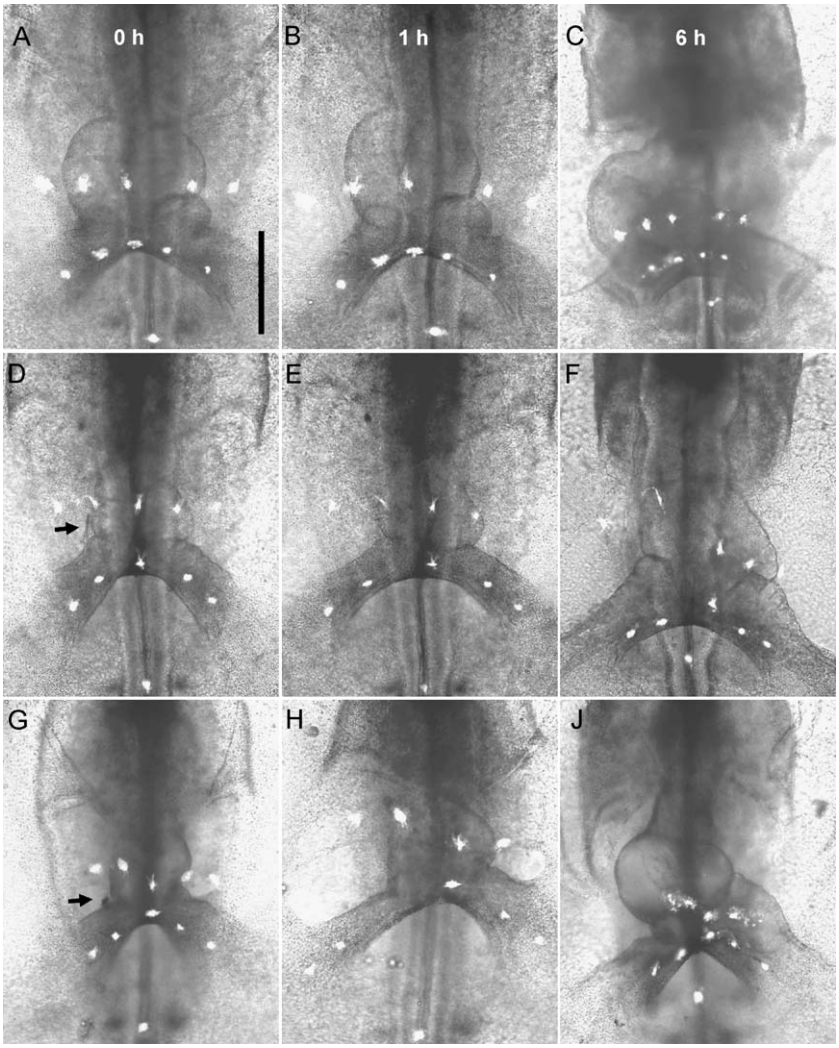

Fig. 7. Influence of local cytochalasin B (CB) exposure on c-looping. Stage 10 embryos were labeled on the splanchnopleure (SPL, upper row of labels), omphalomesenteric veins (OVs), and neural tube at the level of the first pair of somites. (A, D, and G) Beginning of experiment; (B, E, and H) after 1 h of cultivation; (C, F, and J) after 6 h of cultivation. (A–C) Control embryo on surface of culture medium; normal right looping. All labels move closer together due to tissue contraction. (D–F) Embryo on surface of culture medium with CB crystal placed near the rear right side of the heart (indicated by arrow in D); abnormal left looping. Labels on SPL spread apart near crystal, indicating local tissue relaxation; labels in OVs first move apart near crystal (E) and then move together (F). (G–J) Embryo under liquid medium with CB crystal placed near the rear right side of the heart (indicated by arrow in G); right looping. Labels near crystal on SPL spread apart; labels in OVs first move apart near crystal (H) and then move together (J). Scale bar: 400 μm.

looping was observed in all embryos ($n > 200$), the incidence of left looping in treated hearts was significant at the level of $P < 0.001$ (Fisher exact test).

Regional disruption of the actin cytoskeleton

In an intriguing experiment, Itasaki et al. (1991) found that using crystals of cytochalasin B to disrupt myocardial actin on the right side of stage 9–10 chick embryos causes left looping in a significant number of hearts. These results led these investigators to postulate that cytoskeletal contraction within the heart tube determines rotation direction. These experiments, however, were conducted using a culture method that exposes the heart to the effects of surface tension, which can influence the behavior of the heart (Voronov and Taber, 2002). Hence, we repeated these experiments using two culture techniques. The first method places the embryo on an agar surface, exposing the embryo directly to air and the effects of surface tension. The second method places the embryo under a thin layer of fluid that eliminates this potential source of artifact (see Materials and methods).

A crystal of cytochalasin B (Sigma) was applied locally near the rear right caudal side of the stage 10 heart tube through a small hole cut in the SPL (Figs. 7D and G), as in the experiments of Itasaki et al. (1991). (Depending on their size, cytochalasin crystals dissolve completely within 1–3 h of cultivation.) Abnormal left c-looping developed in 68% (6/19) of the embryos cultured on the agar surface (Figs. 7D–F) compared to only 7% (6/89) of control embryos on the surface (Figs. 7A–C). The difference in incidence of abnormal left looping between the treated and control embryos cultured on the surface was statistically significant ($P < 0.001$, chi-square test). However, in all 16 embryos cultured under fluid, right c-looping occurred regardless of application of cytochalasin (Figs. 7G–J).

To help us interpret these results, we placed rows of labels along the SPL and OVs. In control embryos, all labels moved closer together during 6 h of culture (Figs. 7A–C), suggesting that these tissues undergo contraction. In treated embryos, the labels near the CB crystal on the SPL move apart, suggesting local tissue relaxation, while those on the OVs first move apart and then move closer together (Figs. 7D–J). The similarity in these motions for both culture methods indicates that the effects of CB on tissue stress are independent of the presence of surface tension. Hence, we conclude that the differences in looping direction are due to surface tension effects (see Discussion).

Heart development was not completely normal in embryos with cytochalasin applied near the rear part of the heart tube. Fusion of the omphalomesenteric veins was partly suppressed, the heart tube was considerably shorter and often was really not looped, and as a result a cardia bifida-like heart developed. Cardia bifida formed in embryos when the cytochalasin crystal was too large. We discarded such embryos from our results. Itasaki et al. (1991) also discarded some embryos from their data, possibly due to the same reason.

According to the hypothesis of Itasaki et al. (1991), relatively strong circumferential contraction on the right side of the heart tube drives dextral rotation. To further test this idea, we disrupted circumferential tension by cutting the right side of the stage 10 heart tube longitudinally using a fine glass needle that pierced the splanchnopleure (Fig. 8). Following this dissection, c-looping developed (under a layer of fluid) at approximately the same rate and to almost the same extent as in control embryos (Fig. 8C). Due to the presence of the wound, however, the contour of the outer curvature in the cut hearts was not as sharp and distinct as in control embryos (compare Figs. 1B and 8C). The wounds never healed completely even after 6 h of cultivation; instead, they opened widely (Fig. 8D). In contrast, wounds in the splanchnopleure that were created during the heart dissection healed within 1–2 h. All of the dissected hearts looped normally to the right ($n = 23$), suggesting that

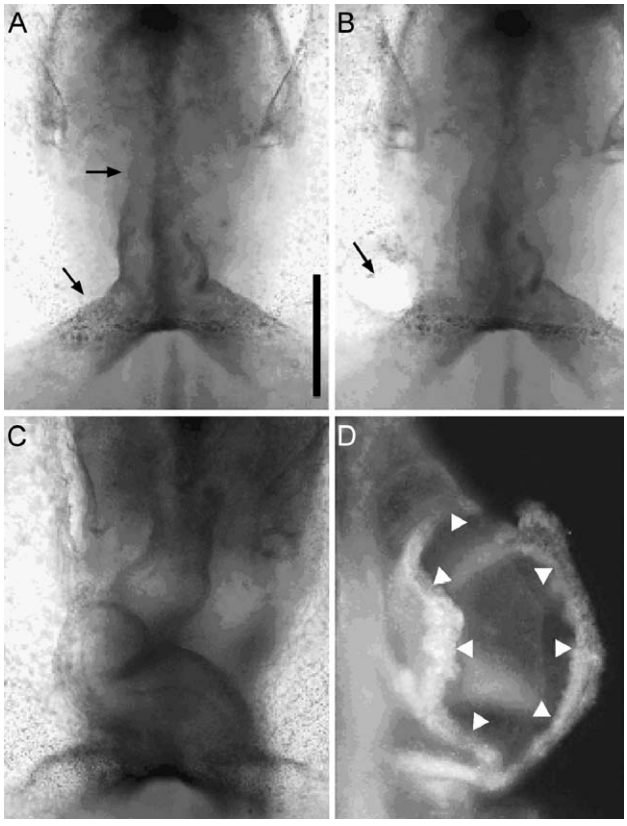

Fig. 8. Development of the heart after longitudinal dissection of myocardium along the right side. (A) Embryo at stage 10+ (9 somites) before dissection (subsequent cut was made between arrows). (B) The same embryo immediately after dissection. Note the fuzzy contour of the right side of heart tube. Arrow indicates the hole in the splanchnopleure through which the dissection was made. (C) The same embryo after 6 h of cultivation; almost normal c-looping. (D) Right side of the dissected heart of the embryo shown in C after actin staining of cytoskeleton. Arrowheads indicate edges of spacious wound, which did not heal after 6 h of cultivation. Scale bar represents 400 μm in A–C and 200 μm in D.

disrupting circumferential tension on the right side of the heart tube does not affect looping direction.

Computational modeling

Our experimental results suggest that both cell migration and cytoskeletal contraction contribute to the stresses in the OVs. To test whether these mechanisms are consistent with the physics of the problem, our computational model was used to simulate looping. Progressive longitudinal contraction and cell migration (growth) were specified along the lower and upper halves of the OVs, respectively (Fig. 9A). In addition, based on recent work focusing on the bending component of c-looping (unpublished results), as well as on observed changes in actin fiber orientation (Itasaki et al., 1989) and MY cell shape during c-looping (Manasek et al., 1972), circumferential and circumferential-longitudinal actin polymerization was specified for the dorsal and ventral halves of the ventricle, respectively (Fig. 9A). In this model of early looping, the force exerted by the SPL was not considered.

Due to the specified forces, the model deforms, with the resulting geometries of the heart and veins resembling those of the stage 10^{+} chick embryo (compare Figs. 4D and 9C). Note the ventral bending and rightward rotation of the heart tube and the change in curvature of the left OV (Figs. 9B and C). The asymmetry that produces rightward rotation in this model is the larger diameter (and hence greater force) of the left OV compared to that of the right OV. In addition, the predicted tensile and compressive stresses, respectively, in the lower and upper parts of the OVs (Fig. 9C) are consistent with our stress data (Fig. 3). Hence, combined cranial-side migration (growth) and caudal-side contraction in the OVs generate morphology and stress distributions that are consistent with the normal heart during early c-looping.

As a further test of this model, the right OV was removed from the initial geometry (Fig. 10A) and the simulation was repeated with everything else left unchanged. Because the contractile stress in the vein developed before stage 9, initial tension in the left OV immediately pulls the caudal end of the ventricle slightly leftward (Fig. 10B). Then, cell migration (growth) in the OV pushes the ventricle toward the right (Fig. 10C). This predicted response agrees quite well with the morphology observed in our corresponding experiment (Figs. 5B and C). In particular, compare the final shape of the left OV in the model and embryo.

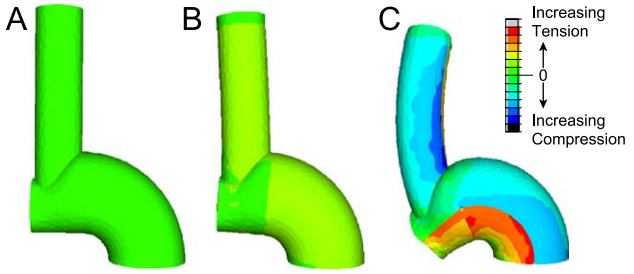

Fig. 10. Computational model of Fig. 9 for stage 10 heart with the right omphalomesenteric vein removed. (A) Original configuration. (B) Immediate deformation due to prior contraction in the caudal region of left vein; caudal end of heart tube displaces leftward. (C) Eighteen hours later; cell influx into vein (modeled as growth) causes rightward deformation. The geometries in B and C are similar to experimental morphology (see Figs. 5B and C). Distributions of longitudinal stress are shown by colors.

Discussion

Results from the present and prior studies suggest that the bending and rotational components of cardiac c-looping are controlled by different sets of forces. While the bending component depends on forces intrinsic to the heart tube (Butler, 1952; Manning and McLachlan, 1990), we have found that the rotational component depends on external forces provided by the SPL and the OVs.

In a previous study, we have found that surface tension may introduce artifact in traditional chick embryo culture preparations. Because this additional force on the embryo is not present in ovo, we developed a new culture technique that excludes the effects of surface tension (Voronov and Taber, 2002). In the present work, this method has allowed us to gain new insights into an old problem.

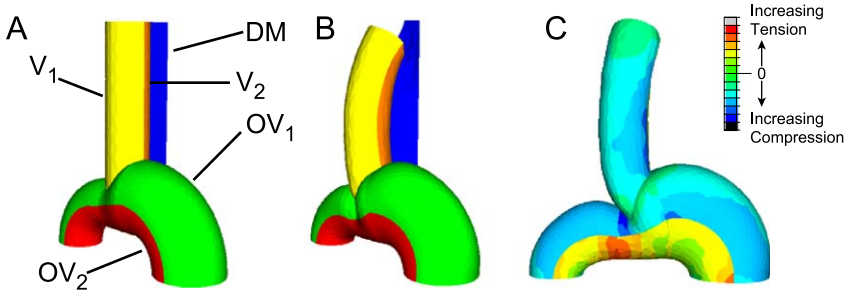

Fig. 9. Computational model for looping heart, including omphalomesenteric veins. (A) Undeformed model (stage 10) showing specified morphogenetic forces. DM = dorsal mesocardium, V_1 = ventral half of ventricle (longitudinal-circumferential polymerization), V_2 = dorsal half of ventricle (circumferential polymerization), OV_1 = cranial half of omphalomesenteric veins (longitudinal growth representing cell migration), OV_2 = caudal half of omphalomesenteric veins (longitudinal contraction). (B) Diagonal view showing ventral bending. (C) Ventral view showing rightward rotation and longitudinal stress distribution (colors). Note the tension and compression in caudal and cranial regions of OVs, respectively.

Forces in splanchnopleure and omphalomesenteric veins drive cardiac rotation

Some investigators have speculated that cardiac rotation during c-looping, like bending, is generated by internal forces in the heart tube. Manasek (1983) and Manasek et al. (1984), for example, have suggested that pressure in the cardiac jelly, combined with a spiraling fiber system in the myocardium, causes the heart tube to twist. However, this hypothesis has been refuted by experiments in which the heart apparently loops normally when the jelly is digested by hyaluronidase (Baldwin and Solursh, 1989). Another hypothesis was offered by Itasaki et al. (1991), who speculated that circumferential contractile forces pull the heart tube rightward, forcing it to rotate about the dorsal mesocardium, which initially anchors the tube to the embryo (Figs. 1A′ and B′). This hypothesis is based on their finding that placing a crystal of cytochalasin B on the left side of the relatively straight stage 9–10 heart tube does not affect looping, but placement on the right side induces abnormal looping to the left. To explain this result, the authors speculated that actin structures in the myocardium undergo a prolonged circumferential contraction that is normally stronger on the right side and, therefore, pulls the heart tube toward the right. If contraction on the right side is disrupted, then the contraction on the left side pulls the heart the other way.

Our experiments have shown, however, that the embryonic chick heart contains little or no intrinsic ability to rotate during c-looping. When both the SPL and OVs are removed from the c-shaped stage 11 heart, the ventricle untwists completely (Figs. 2F–H). Moreover, in a previous study, we observed similar deformation when the SPL was removed from stage 10^{-} embryos at the beginning of the experiment (Voronov and Taber, 2002). During the following 6 h in culture, the heart bent ventrally and dextrally but rotated little.

From these results, we conclude that rotation is caused by forces applied to the heart tube by the SPL and OVs. Long ago, Patten (1922) speculated that the heart is forced to bend to the left or right because of physical impediments supplied by the body of the embryo on the dorsal side and the yolk on the ventral side. The cause of the rightward directionality, however, was not known. Our results are consistent with the idea that physical constraints compel rotation, and, as discussed later, our data also suggest that OVs play a major role in determining directionality.

To find an alternative explanation for the findings of Itasaki et al. (1991), we explored the possibility that their results were affected by surface tension. Hence, we repeated their experiments with and without surface tension present. For embryos cultured in the presence of surface tension, we obtained results similar to theirs, that is, cytochalasin placed near the right side of the heart induced left looping most of the time (Figs. 7D–F). When surface tension was eliminated, however, all hearts looped normally to the right (Figs. 7G–J). Furthermore, in a more direct test of their hypothesis, we disrupted circumferential tension on the right side of the heart by direct mechanical intervention, that is, by cutting the heart longitudinally. This procedure should block force transmission across the right side of the heart, leaving the tension on the left side intact. According to Itasaki et al.'s hypothesis, the cut heart should loop toward the left as in their cytochalasin experiments. However, we found normal rightward c-looping in all treated embryos (Fig. 8).

In a previous investigation (Voronov and Taber, 2002), we repeated the classic experiment of Lepori (1967) and found behavior similar to that in the cytochalasin experiments. When the SPL was cut on the right side of the embryo, the heart usually looped to the left in embryos cultured with surface tension present. This result is consistent with Lepori's study. In similarly treated embryos cultured under fluid, however, most hearts rotated toward the right. We speculated that surface tension increases the friction between the heart tube and the SPL. Hence, when the membrane is cut on the right side, unbalanced tension pulls the SPL toward the left, and, due to elevated friction, the SPL drags the heart also to the left. Without this added friction force, the heart can slide to the right, even as the SPL moves toward the left.

Our present results suggest that the results of Itasaki et al. (1991) can be explained similarly. We speculate that the tension in the SPL is due in part to cytoskeletal contraction of its component cells (see Figs. 7A–C). Diffusion from a cytochalasin B crystal placed under the right side of the SPL disrupts contraction on that side, locally relaxing the membrane (Figs. 7E,F and H,J). Thus, the tension remaining on the left pulls the membrane leftward, and, if surface tension is present, the heart is also pulled to the left (Fig. 7F). Without surface tension present, the heart slides under the SPL to the right (Fig. 7J).

In this context, we also note that cytoskeletal contraction and migration in the right OV could be disrupted by cytochalasin placed near the right side of the heart. Our results suggest, however, that reducing the force in the right OV should not affect looping direction, although, as discussed next, reducing force in the left OV can cause left looping.

Unbalanced forces in omphalomesenteric veins can influence looping direction

Our results indicate that the OVs push in opposite directions against the caudal end of the heart tube. When the right vein is severed, the left vein first pulls the caudal end toward the left and then pushes it rightward (Fig. 5), while cutting the left vein pulls and then pushes in the opposite directions. In agreement with previous speculation (Stalsberg, 1970), these observations suggest that this force imbalance normally biases the caudal end of the straight heart tube to displace toward the right.

We speculate that the net vein force plays a role in looping directionality. This view is supported by results from our experiment in which mesoderm from the left OV was removed while leaving the SPL mostly intact. We reason that this dissection reduces the force in the left vein, allowing the force in the right vein to dominate and push the heart leftward. Indeed, a significant number of these operations resulted in left looping (Fig. 6).

However, 73% of these treated hearts still looped to the right. One reason for this may be that we did not remove enough tissue from the vein. According to our model, looping direction depends on the amount of tissue removed (results not shown). Moreover, other factors, including rightward bending of the ventricle, may provide a rightward bias that the leftward force in the right vein may not be able to overcome. In other words, as suggested by Stalsberg (1970), multiple factors may bias looping toward the right, and disturbing one of them may not be enough to compel looping in the opposite direction.

Cytoskeletal contraction and cell migration may generate the forces in omphalomesenteric veins

To identify the sources of the forces in the OVs, we note the following results. First, labels placed on the OVs at stage 10 normally move toward the heart during c-looping, indicating a general influx of cells into the caudal end of the heart tube (Fig. 4). These cells form the primitive left ventricle and atrium, as the veins progressively fuse in the cranial–caudal direction (de la Cruz, 1998). Second, after global application of cytochalasin B, labels on the caudal sides of the veins move apart within 30 min (results not shown), suggesting relaxation of a contractile state. Third, our tissue-cutting experiments indicate that the cranial and caudal regions of the OVs at stage 10 normally are in states of longitudinal compression and tension, respectively (Fig. 3).

We interpret these results as follows. Under normal conditions, mesodermal OV cells migrate through the OVs as epithelial sheets into the heart using the endoderm as a substrate (Linask and Lash, 1988b). Inward migration alone would cause compression throughout both veins, but longitudinal cytoskeletal contraction in the caudal regions of the veins alters the stress distribution. In fact, our model shows that this combination of contraction and migration produces tension in the caudal parts and compression in the cranial parts of the veins (Fig. 9C), consistent with our observations. Moreover, the predicted deformation pattern is consistent with observed morphological changes under both normal and perturbed conditions (compare Figs. 4D and 9C, and Figs. 5 and 10).

Cytochalasin B inhibits actin polymerization and disrupts the cytoskeleton (Cooper, 1987), leading to loss in both cell motility and contractility (Wakatsuki et al., 2001, 2003). Hence, this drug would be expected to interfere with both stress-generating mechanisms, and, according to our hypothesis, significant cardiac rotation should not occur. In fact, studies have shown that global application of cytochalasin B at sufficient doses can prevent or stop c-looping (Manasek, 1976; Itasaki et al., 1991).

It is important to note that differential growth could also contribute to the stress in OVs. However, arresting mitosis by exposure to colchicine has no discernable effect on c-looping (Icardo and Ojeda, 1984). Moreover, other studies have found no consistent pattern in mitotic rates in the stage 12 heart tube, including the caudal end, which forms from the OVs (Sissman, 1966; Stalsberg, 1969a, 1970). Hence, cell division is an unlikely source of significant OV stress.

The source of left–right asymmetry in the OV forces is not yet clear. Our model suggests that the larger diameter of the left vein can lead to relatively greater force (Fig. 9). However, a difference in contractile strength is also possible.

The cardiac tube bends to the right

Although the primary deformation components of c-looping are ventral bending and rightward rotation (Manner, 2000), the results of our study show that the ventricle actually does bend toward its right side. The magnitude of this dextral bending, however, is substantially smaller than the ventral bending (compare panels B and F with D and H of Fig. 2). Nevertheless, this slight rightward bend may be one of several asymmetries that help guide the heart toward the right side of the embryo.

The cause of the dextral bending is unknown, but we offer two possibilities. The first is based on the work of Stalsberg (1969b), who found that the precardiac regions contribute more cells to the right side of the stage 10^{-} heart tube than the left. The difference between the two sides may be enough to produce the modest amount of rightward bending that we observed.

Regarding the second possibility, we note that when a stage 10 heart is dissected from the embryo, the OVs merge to form a primitive left ventricle and atrium directed toward the right (de la Cruz and Sanchez-Gomez, 1998). Because the outflow tract is fixed, we speculate that the corresponding displacement at the caudal end forces the entire heart tube to bend toward the right. It has been known for some time that, while ventral bending is an intrinsic property of the heart tube (Butler, 1952; Manning and McLachlan, 1990), the shape of the heart during both c-looping and s-looping is affected by the constraints at the ends (Flynn et al., 1991; Manner et al., 1993; Manner et al., 1995). Dextral bending may be one manifestation of these constraints.

In addition, dextral bending appears to contribute to the formation of the interventricular groove on the left side of the heart tube. When the tube straightens after one end of the heart is severed, the groove becomes shallow and almost disappears (Figs. 2C, D, G, and H). As Stalsberg (1970) points out, this mechanism is analogous to bending a finger of an inflated rubber glove.

A hypothetical mechanism for c-looping

Previous hypotheses for the looping mechanism have not proven to be consistent with all available data. Hence, we now present a new hypothesis. Taken together, the results of our experiments suggest the following mechanism for c-looping:

1. Beginning at stage 10, cells in the caudal region of the OVs undergo longitudinal cytoskeletal contraction, which causes tensile and compressive stresses in the caudal and cranial parts of the veins, respectively (Fig. 11A). These stresses pull precardiac cells through the veins toward the caudal end of the heart, possibly inducing additional influx of cells through active migration along lines of stress-aligned fibronectin (Linask and Lash, 1986, 1988a,b; Toyoizumi et al., 1991).
2. Incoming cells in both OVs push against the caudal end of the heart tube, merging to form the primitive left ventricle and atrium. Due possibly to asymmetric vein geometry or contractile strength, the left vein normally pushes with greater force, displacing the heart slightly toward the right (Fig. 11B). The dorsal mesocardium constrains this displacement, converting it into a small rightward rotation about the relatively fixed dorsal side of the heart (Fig. 11B′).
3. Due to its tension, the SPL exerts a compressive force against the ventral surface of the ventricle, pushing it further toward the right as the heart bends toward its original ventral surface and slightly rightward (Fig. 11B′). Actin polymerization likely drives the ventral bending (unpublished results).
4. Further bending and rotation contributes to the rupturing of the dorsal mesocardium, allowing the heart to deform into a c-shaped tube.

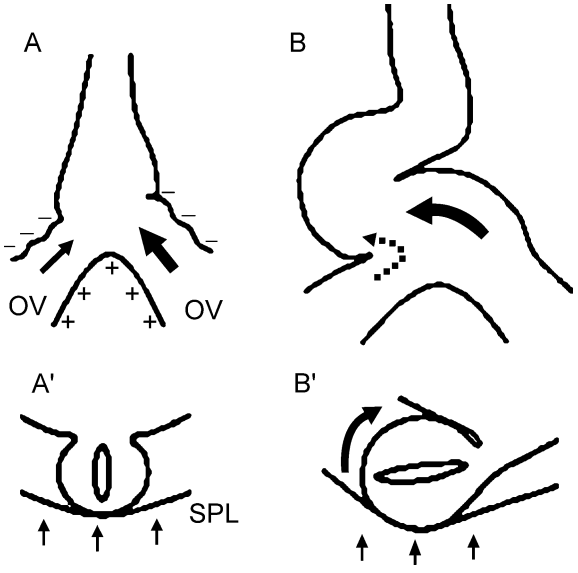

Fig. 11. Schematic of hypothesis for cardiac rotation. (A and B) Ventral view of heart; (A′ and B′) cross-sectional view. (A and A′) Cytoskeletal contraction and cell migration cause compressive (−) and tensile (+) stresses along cranial and caudal surfaces, respectively, of omphalomesenteric veins (OV) of stage 10 embryo as splanchnopleure (SPL) pushes against the ventral surface of the straight heart tube. (B and B′) Relatively greater force in the left vein displaces the caudal end of heart tube toward the right, and the splanchnopleure pushes the heart tube dorsally, increasing rotation magnitude.

While this hypothesis involves considerable speculation, we hope it stimulates new thinking about the looping problem. At the moment, our hypothesis appears to be consistent with available experimental data as well as with fundamental biophysical principles. As data continue to accumulate, however, alternative explanations for our results may surface, leading to alternative conjectures.

Damage to the SPL is a potential source of artifact in some of our experiments. In those experiments in which the SPL was not removed, we tried to minimize the damage as much as possible by inserting the dissection needles through small holes in the SPL. In control tests, we have found that these holes heal relatively rapidly and do not noticeably affect the behavior of the heart during looping. Moreover, we have shown previously that, in the absence of surface tension, the heart loops normally when large cuts are made in the splanchnopleure on either side of the embryo (Voronov and Taber, 2002). Hence, we conclude that such damage did not significantly influence our results.

Dextral looping is a highly conserved process; left looping is a rare event. Hence, redundant mechanisms likely bias looping toward the right side of the embryo (Stalsberg, 1970). The results of the present study suggest that unbalanced OV forces and rightward bending of the cardiac tube may be two such mechanisms. A third may be the rightward pivoting of the conotruncus that occurs in the chick embryo at about stage 13 (Manner, 2000). Within this context, we have observed that partial removal of the left OV sometimes produces hearts that initially loop toward the left but later reverse course to become hearts with apparently normal dextral looping by stage 14 (data not shown). It may be that the right OV initially pushes these hearts leftward, but rightward bending or conotruncal pivoting later forces rotation in the opposite direction.

This study has addressed issues related to the biomechanics of cardiac c-looping. Much work remains to be done on later stages of looping as well as on uncovering the link between genetic and mechanical factors during looping. Discovering this link will require an interdisciplinary effort involving engineers and developmental biologists.

Acknowledgment

This work was supported by NIH grant R01 HL64347 (LAT).

References

Baldwin, H.S., Solursh, M., 1989. Degradation of hyaluronic acid does not prevent looping of the mammalian heart in situ. Dev. Biol. 136, 555–559.

Beloussov, L.V., 1998. The Dynamic Architecture of a Developing Organism: An Interdisciplinary Approach to the Development of Organisms. Kluwer, Dordrecht, The Netherlands.

Beloussov, L.V., Dorfman, J.G., Cherdantzev, V.G., 1975. Mechanical stresses and morphological patterns in amphibian embryos. J. Embryol. Exp. Morphol. 34, 559–574.

Brand, T., 2003. Heart development: molecular insights into cardiac specification and early morphogenesis. Dev. Biol. 258, 1–19.

Bronner-Fraser, M., 1996. Manipulations of neural crest cells or their migratory pathways. Methods Cell Biol. 51, 61–79.

Butler, J.K., 1952. An experimental analysis of cardiac loop formation in the chick. MS Thesis, University of Texas.

Chapman, S.C., Collignon, J., Schoenwolf, G.C., Lumsden, A., 2001. Improved method for chick whole-embryo culture using a filter paper carrier. Dev. Dyn. 220, 284–289.

Cooper, J.A., 1987. Effects of cytochalasin and phalloidin on actin. J. Cell Biol. 105, 1473–1478.

de la Cruz, M.V., 1998. Torsion and looping of the cardiac tube and primitive cardiac segments: anatomical manifestations. In: de la Cruz, M.V., Markwald, R.R. (Eds.), Living Morphogenesis of the Heart. Birkhauser, Boston, pp. 99–119.

de la Cruz, M.V., Sanchez-Gomez, C., 1998. Straight heart tube. Primitive cardiac cavities vs. primitive cardiac segments. In: de la Cruz, M.V., Markwald, R.R. (Eds.), Living Morphogenesis of the Heart. Birkhauser, Boston, pp. 85–98.

Ettensohn, C.A., 1985. Mechanisms of epithelial invagination. Q. Rev. Biol. 60, 289–307.

Flynn, M.E., Pikalow, A.S., Kimmelman, R.S., Searls, R.L., 1991. The mechanism of cervical flexure formation in the chick. Anat. Embryol. 184, 411–420.

Hamburger, V., Hamilton, H.L., 1951. A series of normal stages in the development of the chick embryo. J. Morphol. 88, 49–92.

Harvey, R.P., 1998. Cardiac looping—An uneasy deal with laterality. Cell Dev. Biol. 9, 101–108.

Icardo, J.M., Ojeda, J.L., 1984. Effects of colchicine on the formation and looping of the tubular heart of the embryonic chick. Acta Anat. 119, 1–9.

Itasaki, N., Nakamura, H., Yasuda, M., 1989. Changes in the arrangement of actin bundles during heart looping in the chick embryo. Anat. Embryol. 180, 413–420.

Itasaki, N., Nakamura, H., Sumida, H., Yasuda, M., 1991. Actin bundles on the right side in the caudal part of the heart tube play a role in dextro-looping in the embryonic chick heart. Anat. Embryol. 183, 29–39.

Lepori, N.G., 1967. Research on heart development in chick embryo under normal and experimental conditions. Monit. Zool. Ital. 1, 159–183.

Linask, K.K., Lash, J.W., 1986. Precardiac cell migration: fibronectin localization at mesoderm–endoderm interface during directional movement. Dev. Biol. 114, 87–101.

Linask, K.K., Lash, J.W., 1988a. A role for fibronectin in the migration of avian precardiac cells. I. Dose-dependent effects of fibronectin antibody. Dev. Biol. 129, 315–323.

Linask, K.K., Lash, J.W., 1988b. A role for fibronectin in the migration of avian precardiac cells. II. Rotation of the heart-forming region during different stages and its effects. Dev. Biol. 129, 324–329.

Manasek, F.J., 1976. Heart development: interactions involved in cardiac morphogenesis. In: Poste, G., Nicholson, G.L. (Eds.), Cell Surface in Animal Embryogenesis and Development. North-Holland, New York, pp. 545–598.

Manasek, F.J., 1983. Control of early embryonic heart morphogenesis: a hypothesis. In: Nugent, J., O'Connor, M. (Eds.), Development of the Vascular System. Pitman, London, pp. 4–19.

Manasek, F.J., Burnside, M.B., Waterman, R.E., 1972. Myocardial cell shape changes as a mechanism of embryonic heart looping. Dev. Biol. 29, 349–371.

Manasek, F.J., Kulikowski, R.R., Nakamura, A., Nguyenphuc, Q., Lacktis, J.W., 1984. Early heart development: a new model of cardiac morphogenesis. In: Zak, R. (Ed.), Growth of the Heart in Health and Disease. Raven Press, New York, pp. 105–130.

Manner, J., 2000. Cardiac looping in the chick embryo: a morphological review with special reference to terminological and biomechanical aspects of the looping process. Anat. Rec. 259, 248–262.

Manner, J., Seidl, W., Steding, G., 1993. Correlation between the embryonic head flexures and cardiac development. Anat. Embryol. 188, 269–285.

Manner, J., Seidl, W., Steding, G., 1995. Formation of the cervical flexure: an experimental study on chick embryos. Acta Anat. (Basel) 152, 1–10.

Manning, A., McLachlan, J.C., 1990. Looping of chick embryo hearts in vitro. J. Anat. 168, 257–263.

Markwald, R.R., Trusk, T., Moreno-Rodriguez, R., 1998. Formation and septation of the tubular heart: integrating the dynamics of morphology with emerging molecular concepts. In: de la Cruz, M.V., Markwald, R.R. (Eds.), Living Morphogenesis of the Heart. Birkhauser, Boston, pp. 43–84.

Mercola, M., Levin, M., 2001. Left–right asymmetry determination in vertebrates. Annu. Rev. Cell Dev. Biol. 17, 779–805.

New, D.A.T., 1955. A new technique for the cultivation of the chick embryo in vitro. J. Embryol. Exp. Morphol. 3, 320–331.

Patten, B.M., 1922. The formation of the cardiac loop in the chick. Am. J. Anat. 30, 373–397.

Rodriguez, E.K., Hoger, A., McCulloch, A.D., 1994. Stress-dependent finite growth in soft elastic tissues. J. Biomech. 27, 455–467.

Schock, F., Perrimon, N., 2002. Molecular mechanisms of epithelial morphogenesis. Annu. Rev. Cell Dev. Biol. 18, 463–493.

Sissman, N.J., 1966. Cell multiplication rates during development of the primitive cardiac tube in the chick embryo. Nature 210, 504–507.

Srivastava, D., Olson, E.N., 1997. Knowing in your heart what's right. Trends Cell Biol. 7, 447–453.

Stalsberg, H., 1969a. Regional mitotic activity in the precardiac mesoderm and differentiating heart tube in the chick embryo. Dev. Biol. 20, 18–45.

Stalsberg, H., 1969b. The origin of heart asymmetry: right and left contributions to the early chick embryo heart. Dev. Biol. 19, 109–127.

Stalsberg, H., 1970. Mechanism of dextral looping of the embryonic heart. Am. J. Cardiol. 25, 265–271.

Taber, L.A., 2001. Biomechanics of cardiovascular development. Annu. Rev. Biomed. Eng. 3, 1–25.

Taber, L.A., Perucchio, R., 2000. Modeling heart development. J. Elast. 61, 165–197.

Taber, L.A., Lin, I.E., Clark, E.B., 1995. Mechanics of cardiac looping. Dev. Dyn. 203, 42–50.

Toyoizumi, R., Shiokawa, K., Takeuchi, S., 1991. The behavior and cytoskeletal system of chick gastrula mesodermal cells on substrata coated with lines of fibronectin. J. Exp. Zool. 260, 345–353.

Voronov, D.A., Taber, L.A., 2002. Cardiac looping in experimental conditions: the effects of extraembryonic forces. Dev. Dyn. 224, 413–421.

Wakatsuki, T., Schwab, B., Thompson, N.C., Elson, E.L., 2001. Effects of cytochalasin D and latrunculin B on mechanical properties of cells. J. Cell Sci. 114, 1025–1036.

Wakatsuki, T., Wysolmerski, R.B., Elson, E.L., 2003. Mechanics of cell spreading: role of myosin II. J. Cell Sci. 116, 1617–1625.

Wessells, N.K., Spooner, B.S., Ash, J.F., Bradley, M.O., Luduena, M.A., Taylor, E.L., Wrenn, J.T., Yamada, K.M., 1971. Microfilaments in cellular and developmental processes. Science 171, 135–143.

Zamir, E.A., Srinivasan, V., Perucchio, R., Taber, L.A., 2003. Mechanical asymmetry in the embryonic chick heart during looping. Ann. Biomed. Eng. 31, 1327–1336.